Available online at www.sciencedirect.com
ScienceDirect
Journal of Environmental Sciences 2012, 24(1) 34–49
JOURNAL OF ENVIRONMENTAL SCIENCES
ISSN 1001-0742
CN 11-2629/X
www.jesc.ac.cn

Characteristics and recent trends of sulfur dioxide at urban, rural, and background sites in North China: Effectiveness of control measures

Weili Lin[1], Xiaobin Xu[1,*], Zhiqiang Ma[2], Huarong Zhao[3], Xiwen Liu[4], Ying Wang[1]

1. Key Laboratory for Atmospheric Chemistry, CMA Centre for Atmosphere Watch & Services, Chinese Academy of Meteorological Sciences, Beijing 100081, China. E-mail: linwl@cams.cma.gov.cn
2. Institute of Urban Meteorology, China Meteorological Administration, Beijing 100089, China
3. Institute of Agricultural Mteorology, Chinese Academy of Meteorological Sciences, Beijing 100081, China
4. Wuhan Central Meteorological Observatory, Wuhan 430074, China

Abstract

SO_2 measurements made in recent years at sites in Beijing and its surrounding areas are performed to study the variations and trends of surface SO_2 at different types of sites in Northern China. The overall average concentrations of SO_2 are (16.8 ± 13.1) ppb, (14.8 ± 9.4) ppb, and (7.5 ± 4.0) ppb at China Meteorological Administration (CMA, Beijing urban area), Gucheng (GCH, relatively polluted rural area, 110 km to the southwest of Beijing urban area), and Shangdianzi (SDZ, clean background area, 100 km to the northeast of Beijing urban area), respectively. The SO_2 levels in winter (heating season) are 4–6 folds higher than those in summer. There are highly significant correlations among the daily means of SO_2 at different sites, indicating regional characteristics of SO_2 pollution. Diurnal patterns of surface SO_2 at all sites have a common feature with a daytime peak, which is probably caused by the downward mixing and/or the advection transport of SO_2-richer air over the North China Plain. The concentrations of SO_2 at CMA and GCH show highly significant downward trends (–4.4 ppb/yr for CMA and –2.4 ppb/yr for GCH), while a less significant trend (–0.3 ppb/yr) is identified in the data from SDZ, reflecting the character of SDZ as a regional atmospheric background site in North China. The SO_2 concentrations of all three sites show a significant decrease from period before to after the control measures for the 2008 Olympic Games, suggesting that the SO_2 pollution control has long-term effectiveness and benefits. In the post-Olympics period, the mean concentrations of SO_2 at CMA, GCH, and SDZ are (14.3 ± 11.0) ppb, (12.1 ± 7.7) ppb, and (7.5 ± 4.0) ppb, respectively, with reductions of 26%, 36%, and 13%, respectively, compared to the levels before. Detailed analysis shows that the differences of temperature, relative humidity, wind speed, and wind direction were not the dominant factors for the significant differences of SO_2 between the pre-Olympics and post-Olympics periods. By extracting the data being more representative of local or regional characteristics, a reduction of up to 40% for SO_2 in polluted areas and a reduction of 20% for regional SO_2 are obtained for the effect of control measures implemented for the Olympic Games.

Key words: SO_2 trend; North China; pollution control; Beijing Olympic Games
DOI: 10.1016/S1001-0742(11)60727-4

Introduction

SO_2 is an important gas in atmosphere with climate (Ward, 2009) and environmental significance (Seinfeld and Pandis, 2006). Anthropogenic SO_2 is mainly emitted from fossil fuel combustion, and it also comes from the transformation of precursors emitting from ocean, volcanic emission, organic corruption, and other natural emissions (Slanina et al., 2006). Through diffusion/dilution and chemical transformation into sulfate aerosols in the atmosphere, SO_2 can have significant effect on global and regional climate change and atmospheric chemistry (Kiehl and Briegleb, 1993; Mitchell et al., 1995; Ravishankara, 1997). When the concentration of SO_2 exceeds critical levels, it may have adverse effects on human health and crops (WHO, 2000). Sulfate particles in the atmosphere are effective cloud condensation nuclei (Manktelow et al., 2009). The global scale increase in the number of cloud condensation nuclei would result in an increase in cloud albedo and the increase of sulfate particles can increase the intensity of solar radiation reflected back to the space (Kaufman et al., 2002; Alexander et al., 2005). SO_2 also plays an important role in acid deposition. When returning to ground via dry and wet deposition, SO_2 and its products, such as sulfuric acid and sulfate particles, will increase the acidity of settlement areas, and thus incur damage to sensitive ecosystems (Seinfeld and Pandis, 2006).

Coal is the main energy source in China. The huge demand on coal, together with its high sulfur content and poor coal processing and burning technique makes China the largest SO_2 emission source in the world (Stern, 2005). In 2006, China's total SO_2 emission was 25.888 million tons, and increased 1.5% compared with that in 2005 (State Environmental Protection Agency, Environmental Statistics Yearbook 2006). SO_2 emission is the most

* Corresponding author. E-mail: xuxb@cams.cma.gov.cn

important cause of acid deposition in China (Larssen et al., 2006). Acid rain monitoring results showed that about 30%–40% of the Chinese territory experienced acid rain, making China the world's 3rd largest acid rain area after the North America and Europe (Wang and Ding, 1997; Wang and Wang, 1995; Tang et al., 2010). SO_2 is also one of the most important pollutants and one of the key precursors of secondary aerosols in ambient air in China's major cities and economic regions. Thus, it is important to observe and study the emission and ambient concentration of SO_2 in China. Recently, the trend of SO_2 observed at two regional atmosphere background stations in China has been analyzed by Xu et al. (2009a). The results showed that sulfur pollution had been as severe as that in the middle 1990s and there were no significant changes in surface SO_2 concentrations over the Yangtze River Delta region in the period 1995–2006, and SO_2 level increased at an annual rate of 22.2% over the Northeast China Plain region. With the implementation of the strategic plan of developing Western China, the surface SO_2 concentrations at such clean regions as the Qinghai-Tibet Plateau and other economically underdeveloped areas also raise concerns.

There are dense population and intensive agricultural and industrial activities in the North China plain. Near-surface monitoring results (Thornton et al., 1997; Ding et al., 2009; Meng et al., 2009; Lin et al., 2009), pollutant emissions estimation (Streets and Waldhoff, 2000; Zhang et al., 2009a; Lu et al., 2010) and satellite retrieval results (Krotkov et al., 2006) show that Northern China is one of the most heavily polluted areas in the world with high anthropogenic SO_2 emission and pollution, which have great impact on the air quality in the area and its surrounding and make great contributions to acid deposition and global sulfur burden (Lee et al., 2008; Carmichael et al., 2002; Shao et al., 2006; Fiedler et al., 2009). As the SO_2 pollution control measures continue to tighten, China's SO_2 emission began to decrease in 2006. However, it still maintains a higher level, and the SO_2 emission in 2007 was still 49% higher than that in 2000 (Lu et al., 2010). SO_2 emissions in North China decreased from 2006 also, but the total emission is still at a high level and the major emission sources are power plants and industrial activities (Lu et al., 2010). Beijing's air quality problems were characterized historically by high concentrations of particulate matter and SO_2 (Hao and Wang, 2005). According to the result of surface observations, annual average concentration of SO_2 in Beijing urban area has dropped significantly since 1998 (Zhang et al., 2006). In 2006, the annual average concentration of SO_2 in Beijing urban area was (22.5 ± 22.1) ppb (Ji et al., 2009) and in the clean background station, Shangdianzi was (7.6 ± 5.1) ppb (Meng et al., 2009). The mean value of SO_2 was (17.1 ± 12.8) ppb at Gucheng, a rural site close to Beijing, during July 2006–September 2007 (Lin et al., 2009). In the heating season, SO_2 concentrations were 3–6 times higher than that in non-heating period (Zhang et al., 2006; Ji et al., 2009). The SO_2 concentrations in Beijing and its surrounding areas are still relatively high. As the regional atmospheric oxidizing capacity increases (Lin et al., 2008), the total suspending particles decrease, the ability of the primary particulate matter to neutralize the acidity of the precipitation weakens, and the concentration and ratio of secondary particles such as sulfate and nitrate, increase, the frequency of acid rain in Beijing and its surrounding area has significantly increased in recent years (Tang et al., 2007; Zhao and Hou, 2010).

Therefore, it is important to understand the variation and trend of SO_2 in North China in recent years. It has also been one of the scientific interests to quantify the effectiveness of SO_2 control measures in and around Beijing, which have been implemented in the recent years, particularly for improving the air quality during the Beijing 2008 Olympic Games. In this article, we show surface SO_2 measurements made at different types of sites in North China in recent years, analyze the variations and trends of SO_2, and quantify the effectiveness of pollution control measures.

1 Observations

The observational data of SO_2 are mainly from 3 sites, i.e., the Shangdianzi site (SDZ; 40.65°N, 117.12°E, 293.9 m a.s.l.), the China Meteorological Administration site (CMA; 39.95°N, 116.32°E, 96 m a.s.l.), and the Gucheng site (GCH; 39.13°N, 115.12°E, 15.1 m a.s.l.). These sites represent the background area (SDZ), Beijing urban area (CMA), and the relatively polluted rural area (GCH), respectively. Geographically, these 3 sites align along the northeast-southwest line and are situated east of Taihang Mountains (Fig. 1). To extend the time series of data for Beijing urban area, SO_2 data during January–November, 2007 from the Baolian site (BL; 39.93°N, 116.28°E, 75.0 m a.s.l.), a site 2.9 km southwest to CMA, are combined with those from CMA to represent the SO_2 data in the urban area. In addition, about 7 months of observational data collected at the Wuqing site (WQ; 39.39°N, 117.02°E, 5 m a.s.l.), which is located between Beijing and Tianjin, are also used in this study. Figure 1 shows the geographic distribution of the observation sites and their neighboring cities. Some meteorological data from these sites are used in this article to facilitate the analysis.

The observation at CMA site was made on top of a

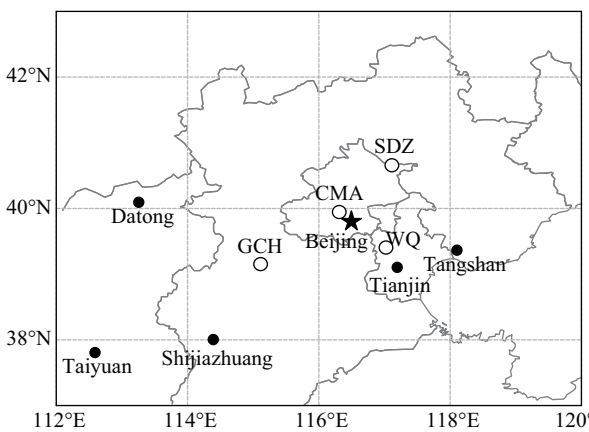

Fig. 1 Geographic distribution of observation sites (hollow circles) and nearby cities (solid circles).

building (38 m above ground level) in the yard of CMA. The site is located in the northwest of Beijing urban area. The distances from the site to the western arteries road (Zhongguancun Nandajie), to the west 3rd ring road, and to the north 3rd ring are 0.45 km, 1.7 km, and 1.9 km, respectively. More information on the CMA and BL sites and the analysis of part of the observational data can be seen in previous publications (Zhang et al., 2009b; Lin et al., 2011b).

The GCH site is an Integrated Ecological-Meteorological Observation and Experiment Station affiliated to Chinese Academy of Meteorological Sciences, located in Hebei Province. The site is about 110 km to the southwest of Beijing, 130 km to the west of Tianjin municipality (population about 10.75 million), 35 km to the north of Baoding (population about 1.05 million), and 160 km to the northeast of Shijiazhuang (population about 9.55 million). Previous studies (Lin et al., 2009) have shown that this site has good regional representativeness. The SO_2 data from GCH cover the periods August 2006–August 2007 and June 2008–January 2010. Details about the measurement were described by Lin et al. (2009).

The SDZ site is one of the regional background stations in China and is a WMO/GAW regional station. The station is located in the northern part of North China Plain and in Miyun County of Beijing. It is about 100 km and 55 km northeasterly to the urban area and Miyun Township, respectively. Within 30 km of the site, there are only small villages in mountainous areas with sparse population and thus insignificant anthropogenic emission sources. The observation building of the station is situated on the south slope of a hill, on the north side of a valley with a northeast-southwest orientation. The southwest mouth of the valley is open to Beijing and the North China plain. SO_2 data from SDZ for September 2004–December 2009 are used in this study.

The WQ site is located at the Wuqing Meteorology Station, Wuqing Town, Tianjin Province. Wuqing Town, with inhabitants of about 0.8 millions, is a relatively less densely populated area between two megacities, Beijing and Tianjin. There are some plants of light industry about 2 km away from the site and a major road nearby. In the north, west and southwest of the observation site, large areas are covered by farmlands, with railways and busy roads running through. The center Wuqing Town locates east of the WQ sites. Observation at WQ was carried out from July 2009 to January 2010 (Xu et al., 2011).

The SO_2 mixing ratio was measured using the pulsed fluorescence method. The instrument types are 43CTL SO_2 analyzer (Thermo Environmental, USA) for SDZ, CMA, WQ, and GCH, and 9850B SO_2 analyzer (Ecotech, Australia) for Baolian (BL). Zero and span checks were routinely carried out daily or weekly. Multi-point calibrations were done monthly. The SO_2/N_2 standard mixtures used at the sites for *in situ* calibrations were produced by different factories and in different time. The differences among the standards can be significant (Lin et al., 2011a) and were determined by comparing with the same NIST-traceable SO_2 standard produced by Scottgas, USA.

Table 1 Monthly and annual mean concentrations (AVG) and their standard deviation (STD) of SO_2 observed at CMA, GCH, WQ, and SDZ

Month	CMA (ppb)		GCH (ppb)		WQ (ppb)		SDZ (ppb)	
	AVG	STD	AVG	STD	AVG	STD	AVG	STD
Jan	40.9	8.0	32.2	9.4	31.2	23.2	12.2	2.1
Feb	35.3	16.7	24.2	11.2			13.0	2.5
Mar	20.5	6.0	15.8	1.4			10.2	1.3
Apr	9.2	4.8	10.8	0.9			7.7	2.1
May	7.6	2.7	9.4	0.2			5.7	1.5
Jun	6.9	2.9	8.8	3.5			4.0	1.7
Jul	6.0	2.2	6.0	2.2	6.7	6.2	1.6	0.6
Aug	5.4	1.9	5.8	2.1	4.9	6.2	2.2	0.4
Sep	6.8	1.5	7.1	2.0	11.2	8.3	4.5	1.5
Oct	7.7	0.7	9.7	2.4	12.7	12.0	6.5	2.9
Nov	22.1	2.4	17.7	4.3	23.1	20.3	9.3	0.6
Dec	33.0	7.1	30.6	9.8	26.7	22.4	12.6	1.4
Annual	16.8	13.1	14.8	9.4	–	–	7.5	4.0

–: no enough monthly mean data can be used to calculate the annual mean.

2 Variations of surface SO_2

2.1 Seasonal variations

Figure 2 shows the variations of the monthly average SO_2 concentration in different years at the 4 sites. They all show "U" shaped distributions with much higher SO_2 concentrations in winter (heating period) and lower SO_2 concentrations in summer. The monthly and annual statistics of SO_2 concentrations observed at the 4 sites are shown in Table 1. At CMA, GCH, WQ, and SDZ, the average SO_2 concentrations are 36.4, 29.0, 29.0 and 12.6 ppb in winter (DJF), respectively, and 6.1, 6.9, 5.8 and 2.6 ppb in summer (JJA), respectively, with the winter/summer ratios of 6.0, 4.2, 5.0 and 4.8, respectively. The highest SO_2 concentration is found at CMA, the urban site of Beijing, followed by GCH and WQ, and the lowest one is at SDZ, the regional background site of North China. According to China's "Ambient Air Quality Standard" (GB3095-1996), the annual average concentrations of SO_2 at CMA and GCH are lower than the Grade II standard value (22.8 ppb) but higher than the Grade I standard value (7.6 ppb) and the annual average concentration at SDZ station is close to the Grade I standard value (7.6 ppb).

2.2 Diurnal variations

Figure 3 shows the average diurnal variations of SO_2 concentrations at the 4 sites during the observation period. Usually, the first trough of SO_2 concentration appears at 6:00 (WQ at 4:00), and then the concentration gradually increases and reaches the peak during the daytime. At different sites, the daytime concentration of SO_2 peaks at different times of day. It peaks around 15:00–16:00 at SDZ, around 10:00–11:00 at WQ, at 11:00 at GCH, and at 9:00 at CMA. After peaking, the SO_2 concentration at all sites begins to decline. SO_2 at WQ and CMA reaches the second trough at 16:00 and then increases again and reaches the second peak at 24:00, while SO_2 at SDZ and GCH keeps deceasing after 16:00 till 6:00 of next morning. The daytime peak level of SO_2 is always the daily maximum except for the wintertime SO_2 at CMA, which shows nighttime

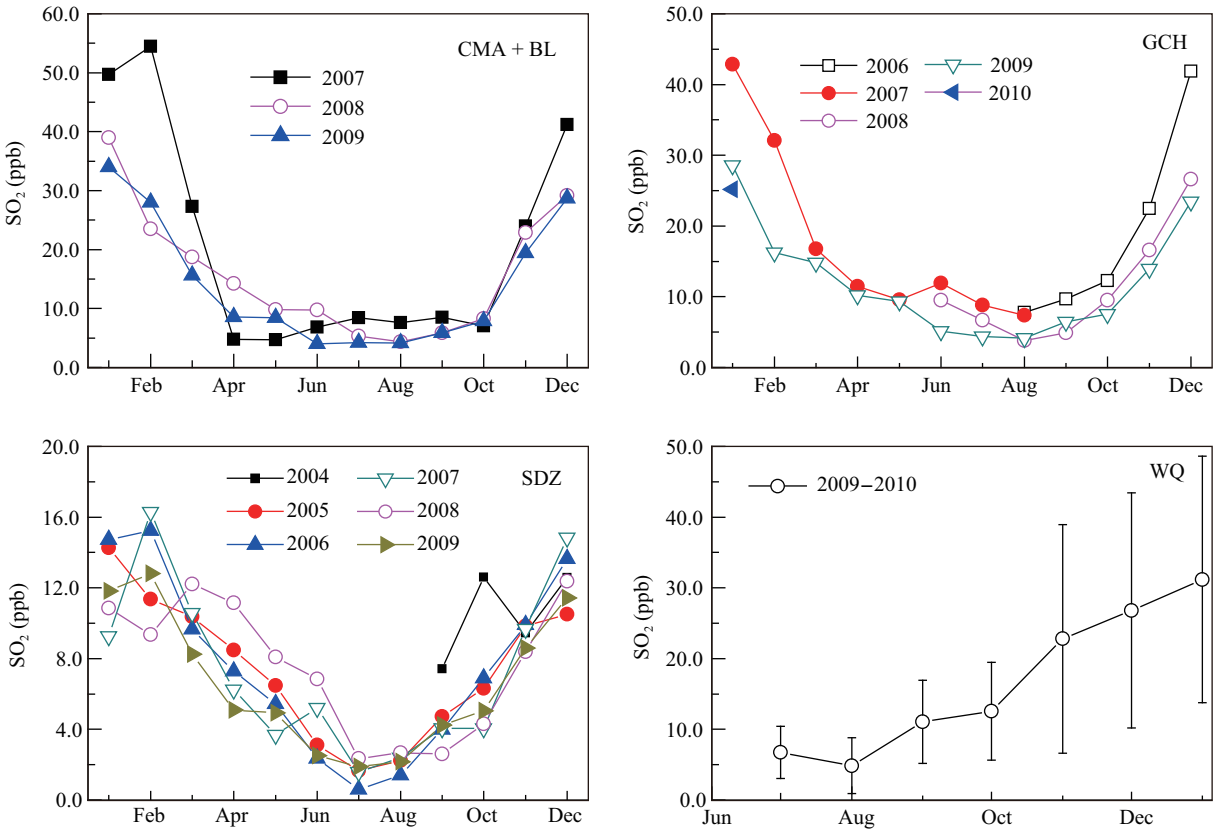

Fig. 2 Variations of the monthly average SO_2 concentrations in different years at CMA + BL, GCH, WQ, and SDZ.

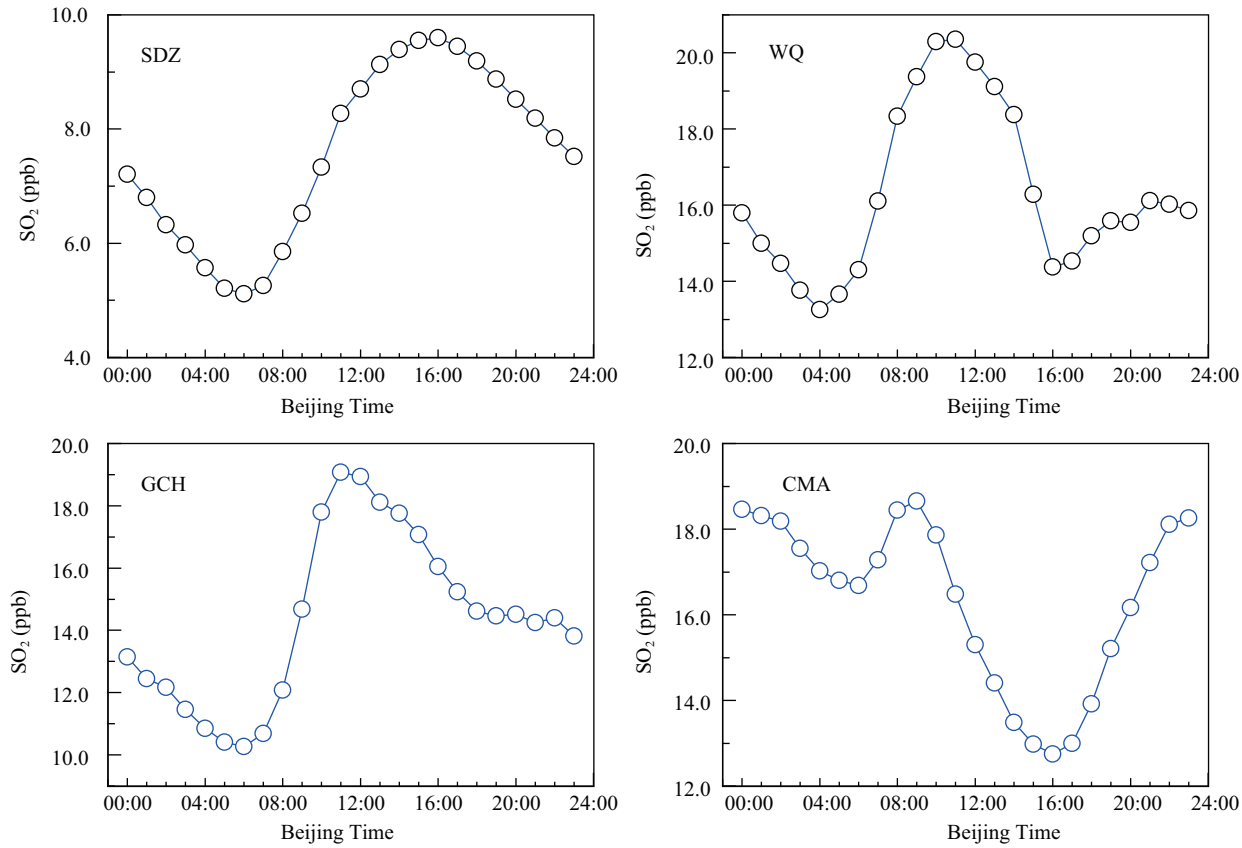

Fig. 3 Average diurnal variations of SO_2 at SDZ, WQ, GCH, and CMA during the observation period.

maximum. Diurnal patterns with daytime SO_2 peak are also reported for some other sites in Beijing, where short-term observation was carried out (Meng et al., 2009a). The daytime peak seems to be regional phenomenon of surface SO_2 in the Northern China Plain. This phenomenon can be attributable to advection transport and/or downward

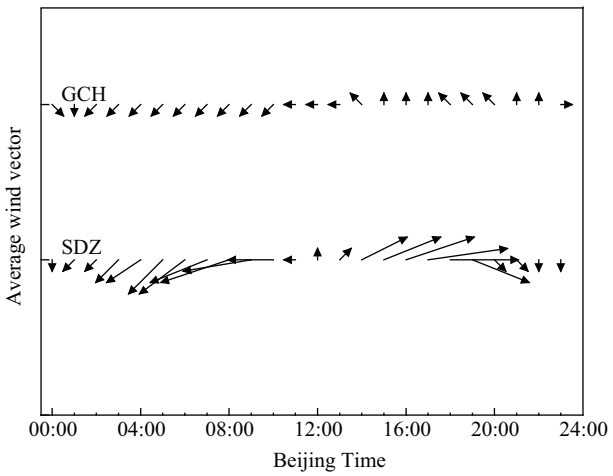

Fig. 4 Average diurnal variation of wind vector at GCH and SDZ.

mixing of SO_2-richer air.

The most significant influence by the advection transport appeared at the sites of SDZ and GCH. Due to the mountain-plain topography, the diurnal changes in wind direction at SDZ and GCH show a regular pattern, as shown in Fig. 4. Around noon, the wind changes from the northerly to southerly. At GCH, such change usually leads to higher concentrations of SO_2 (Lin et al., 2009). At SDZ, pollutants from the south area of Beijing and its surrounding areas can significantly affect the background levels (Lin et al., 2008; Meng et al., 2009b). Therefore, the advection transport of SO_2 from the polluted areas in the afternoon can be an important cause for the maintenance of the high SO_2 level at SDZ and GCH.

The premise for the phenomenon of the high surface SO_2 due to convective transport is that the SO_2 concentration in the elevated layers is higher than that near the ground. During the development of convective process, the higher concentration of SO_2 in the higher layer of air can be exchanged towards the ground, resulting in near-surface high SO_2 concentration. The difference in the time when the peak values appeared shall reflect the difference in the height where the higher concentration of SO_2 stayed and the difference in the development of the mixing height in different days and at different sites. Some observations showed that there existed different SO_2 concentration layers over North China. Measurements at a 325 m height tower in Beijing urban area found that the vertical distribution of SO_2 concentration showed features of layered distribution with lower concentration at the near-ground layer and high concentrations in the higher layers during the non-heating season (Sun et al., 2006; Sun et al., 2009; Meng et al., 2008). As early as 1998, the results of aircraft observations over North China (Tang et al., 2000) showed that there existed high levels of SO_2 and NOx layer at the height of about 1.5 km. Chen et al. (2009) reported the results of aircraft observations on August 18, 2007 in Beijing and showed that there existed a high pollution level in the 2500–3500 m height in the air, where the SO_2 concentration were 1–2 times higher than that near the ground. Xue et al. (2010) reported very high concentrations of SO_2 in the plains of central-eastern China, especially in Shandong, where an averaged SO_2 of up to 51 ppb was observed in the planetary boundary layer by aircraft measurements in October 2007. However, their results do not show the elevated layer of high SO_2, suggesting that the elevated layer may occur mainly over the north part of the North China Plain. With the elevation of the mixing layer height, the higher SO_2 at higher altitudes can be transported downwards to the surface layer by convective process, leading to peak of near ground SO_2 during daytime.

2.3 Variability of hourly and daily mean SO_2 concentrations

Figure 5 shows the frequency distributions of hourly average SO_2 concentrations at 4 sites. It can be seen that the frequencies of low SO_2 levels are dominant at each site and all frequency distribution curves have a prolonged tail at high level end. Therefore, all sites, including the regional background site SDZ, were subject to high levels of SO_2 pollution although the SO_2 level at the sites was relatively low for most of the observation periods. Strong seasonal, diurnal, and wind-related variations of SO_2 are main causes for the frequency distributions.

At CMA, the daily mean SO_2 concentration varied in the range of 0.2–97.6 ppb, with 29 of the 764 observation days having the levels higher than 57 ppb (Grade II of China's Ambient Air Quality Standard for 24 hr) and 4 days higher than 95 ppb (Grade III standard for 24 hr). The hourly mean SO_2 concentration varied in the range of (0–147.3) ppb, with all having the levels lower than 190 ppb (Grade II standard for 1 hr) and 1,003 of the total 18,162 hr (5.5%) having the levels higher than 57 ppb (Grade I standard for 1 hr).

At SDZ, the daily mean SO_2 concentration ranged from 0.1 to 47.7 ppb, with all of the 1905 observation days having the levels lower than 57 ppb (Grade II standard for 24 hr) and 194 days having the levels higher than 19 ppb (Grade I standard for 24 hr). The hourly mean SO_2 concentration ranged from 0 to 93.1 ppb, with all having the levels lower than 190 ppb (Grade II standard for 1 hr) and 174 hr of the total 45,154 hr (0.4%) having the levels higher than 57 ppb (Grade I standard for 1 hr).

At GCH, the daily mean SO_2 concentration was in the range of (0.3–84.8) ppb, with 15 days of the 1024 observation days having the levels higher than 57 ppb (Grade II standard for 24 hr) and 151 days having the levels higher than 19 ppb (Grade I standard for 24 hr). The hourly mean of SO_2 concentration was in the range of 0–143.8 ppb, with all having the levels lower than 190 ppb (Grade II standard for 1 hr) and 825 hr of the total 24,918 hr (3.3%) having the levels higher than 57 ppb (Grade I standard for 1 hr).

At WQ, the daily mean SO_2 concentration varied from 0.0 to 137.7 ppb, with 3 days of the 197 observation days having the values higher than 57 ppb (Grade II standard for 24 hr) and 55 days having the values higher than 19 ppb (Grade I standard for 24 hr). The hourly mean of SO_2 concentration varied from 0 to 147.3 ppb, with all having the levels lower than 190 ppb (Grade II standard for 1 hr)

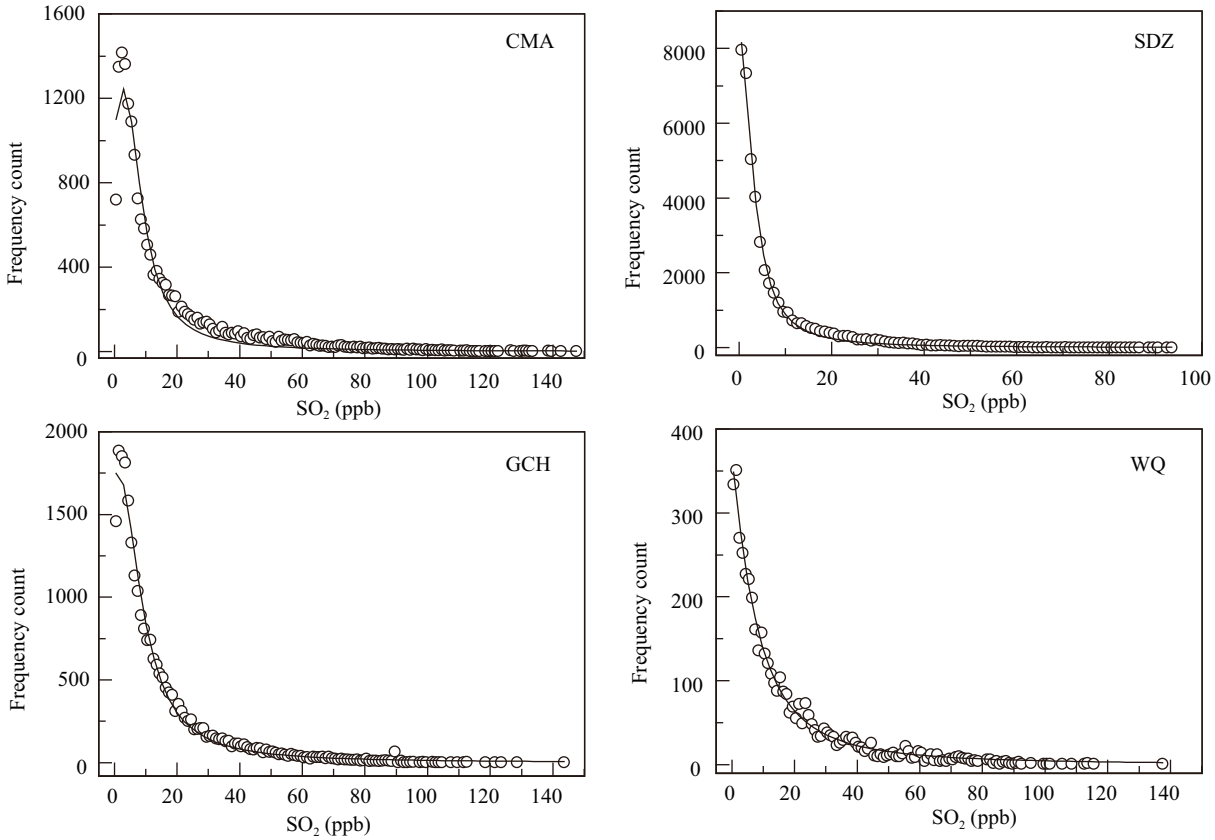

Fig. 5 Frequency distributions of hourly average SO_2 concentrations at CMA, SDZ, GCH, and WQ.

and 215 hr of the total 4539 hr (4.7%) having the values higher than 57 ppb (Grade I standard for 1 hr).

2.4 Regional characteristics

Figure 6 shows the relationships among the daily mean SO_2 concentrations at 4 sites. It can be seen from the figure that strong correlations ($P < 0.0001$) exist, indicating the regional characteristics of SO_2 pollution in North China. Previous research results of Xu et al. (2005) suggest that NOx, CO, and SO_2 in urban boundary layer of Beijing not only varied synchronously in space, but also showed an "in-phase" evolution feature in time. Meng et al. (2009a) analyzed SO_2 observation data at three different sites in Beijing and its surrounding area and found that the daily SO_2 concentrations changed greatly day by day and usually had the same trend at different sites under the control of the same weather systems, indicating a regional distribution of SO_2 pollution. The results of satellite observation clearly show a regional distribution of severe SO_2 pollution over the North China region (Krotkov et al., 2006).

3 Impact of control measures on surface SO_2

3.1 General trends of SO_2

The time series of daily average SO_2 concentrations in the recent years at CMA, GCH and SDZ are showed in Fig. 7. Linear fitting on the results shows that the surface concentrations of SO_2 at CMA and GCH have a very significant downward trend (P <0.0001; –4.4 ppb/yr for CMA and –2.4 ppb/yr for GCH), and the SO_2 concentration at SDZ has a much smaller downward trend (P< 0.05; –0.3 ppb/yr) but it is not as significant as those at CMA and GCH. According to the historical monitoring data from Beijing, the annual average concentration of SO_2 showed an upward trend during 1983–1998, but a downward trend during 1998–2006 (Zhang et al., 2006; Ji et al., 2009). An annual average SO_2 concentration of 22.5 ppb was reported for Beijing urban area in 2006 (Ji et al., 2009), and the present study shows that the annual average concentrations of SO_2 in Beijing urban area are 21.4, 15.9 and 14.1 ppb in 2007, 2008 and 2009, respectively. The average SO_2 concentration at GCH is 19.0 ppb from August 2006 to July 2007 and 12.5 ppb from August 2008 to July 2009, indicating a significant decrease in recent years.

The annual average of SO_2 concentrations at SDZ in 2005, 2006, 2007, 2008, and 2009 are 7.4, 7.6, 7.3, 7.6, and 6.6 ppb, respectively. The annual average concentration of SO_2 at SDZ shows small year-to-year fluctuations and does not have the same significant downward trend as those at CMA and GCH. Since SDZ is a regional GAW station, data from this site reflect more regional characteristics and trends of the average state of the atmosphere than the other observation sites. A small trend in the regional background may be masked by influences of local emission or meteorological conditions. In order to reduce as much as possible the influence of local emission and the impact of the change of the mixing layer height, we analyzed the SO_2 data between 14:00–16:00 in the afternoon, when the boundary layer is well developed and local emission

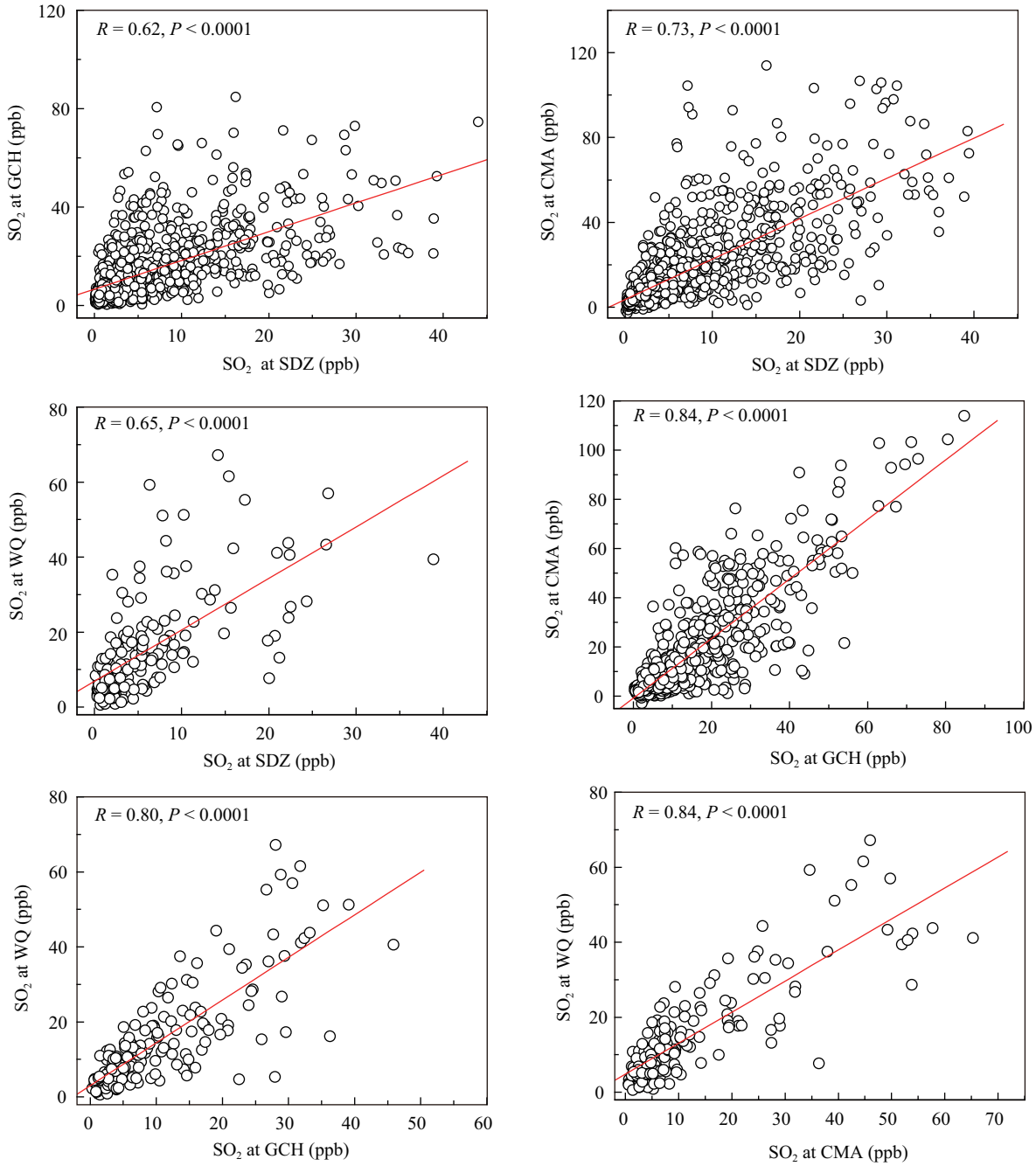

Fig. 6 Correlations among the daily means of SO_2 at the 4 sites.

is assumed to have least impact on the observation. The SO_2 concentration during this time period should better represent the regional situation and shows a downward trend of –0.4 ppb/yr from 2005 to 2009, which is nearly the same as that derived from all data.

3.2 Impact of control measures for 2008 Olympic Games

3.2.1 An overview

In addition to the nation-wide control measures, much more effective and stricter pollution control measures were implemented in North China prior to and during the 2008 Olympic Games in Beijing. The significant reduction of SO_2 in Beijing during the Olympics was proved by the results of emission calculations and *in-situ* monitoring data (Wang et al., 2009, 2010; Zhang, 2009a). SO_2 is mainly emitted from the coal-burning. The implementation of SO_2 control technology has long-term benefits, so that the reduction of SO_2 is effective not only for the Olympic period but also for the post-Olympic period. Here, the pre-Olympic period (pre-Olympics; before August 1, 2008) and the post-Olympic period (post-Olympics; after August 1, 2008) are defined. Figure 8 shows the average diurnal variations of SO_2 at CMA, SDZ and GCH before, during and after the Olympics. As can be seen, the SO_2 concentrations in the post-Olympic period are significantly lower than those in the pre-Olympic period at the three sites. On average, the SO_2 concentrations are reduced by 26%, 20% and 28% at CMA, SDZ and GCH site, respectively. In the following sections, we will analyze the change of SO_2 in

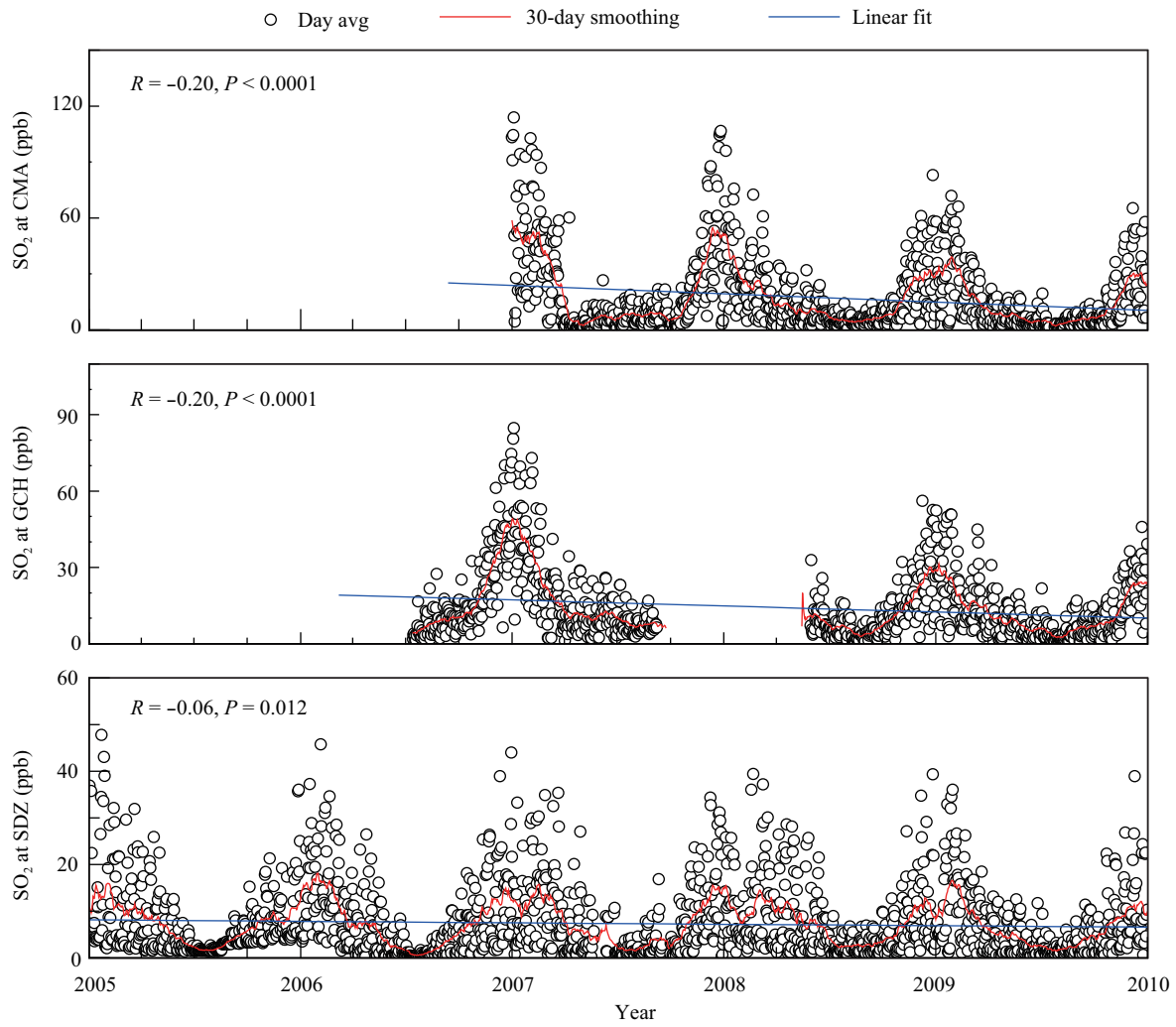

Fig. 7 Time series changes of daily mean SO_2 and trends in recent years at CMA, GCH and SDZ.

the pre-Olympics and post-Olympics from different points of view and try to get a quantitative assessment on SO_2 pollution control measures.

3.2.2 Changes of SO_2 at CMA

Figure 9 shows the monthly average and the relative frequency distribution of hourly mean of SO_2 concentrations during the pre-Olympic and post-Olympic periods at CMA. The annual average concentration of SO_2 is (19.3 ± 15.7) ppb during the pre-Olympic period and (14.3 ± 11.0) ppb during the post-Olympic period. The greatest decrease in the absolute SO_2 concentrations appeared in winter, especially in December with a reduction of 17.7 ppb (38%). The frequency of high SO_2 concentrations (>70 ppb) is also significantly reduced (Fig. 9b). In August, the mean concentration of SO_2 is 7.6 ppb during the pre-Olympic period and 4.3 ppb during the post-Olympic period. Wang et al. (2009) compared the afternoon SO_2 concentrations when the winds came from SSW-SW-S directions in August 2007 (mean value of 6.2 ppb) with those in August 2008 (2.4 ppb) at the observation site in Miyun (116°46.45′E, 40°29′N) and found that the SO_2 concentration was reduced by 61% during the Olympics. Wang et al. (2010) reported a reduction of 41% of SO_2 emission during the Olympic Games when comparing with

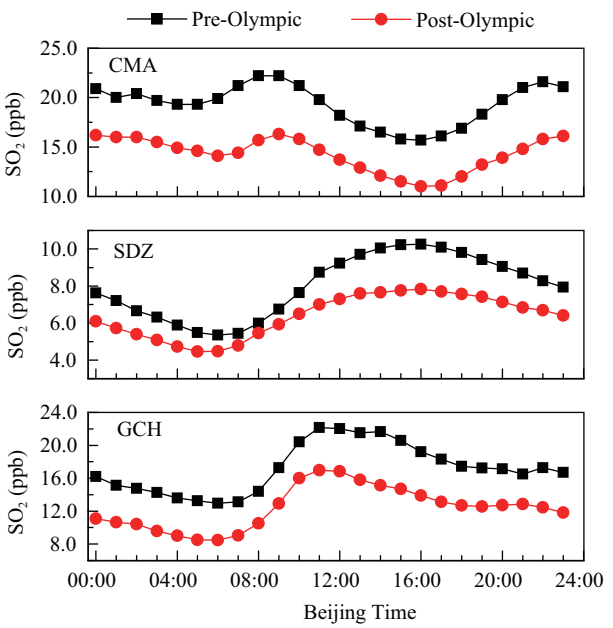

Fig. 8 Average diurnal variations of SO_2 in the pre-Olympics and post-Olympics at CMA, SDZ and GCH.

the emission levels in June 2008. It is noteworthy that SO_2 concentrations in May and October do not show decrease (but increase) after the Olympics. The reason

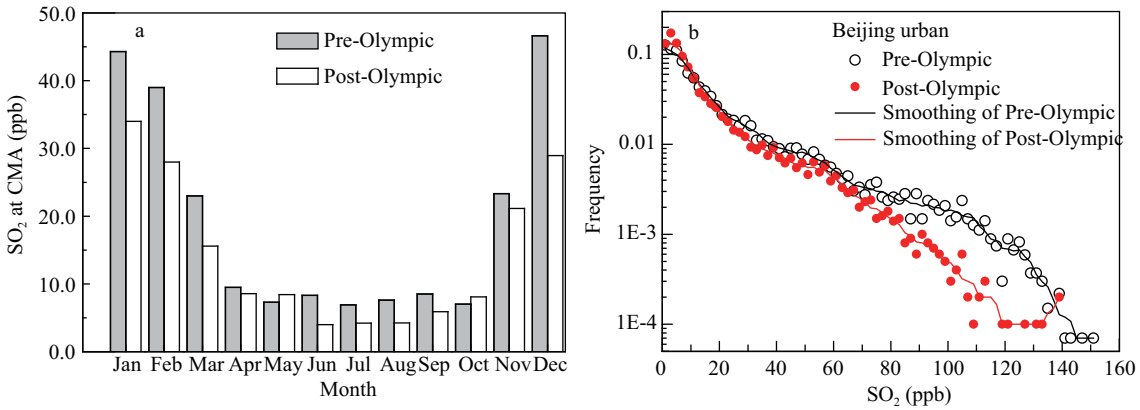

Fig. 9 Monthly mean (a) and the frequency distribution of hourly mean (b) of SO_2 concentrations in the pre-Olympics and post-Olympics at CMA.

for this is unclear. The decrease of SO_2 in November is not as much as that in winter, which might be mainly due to the variation of the actual starting date of heating (usually on November 15) in different years because the starting date is often adjusted according to the weather conditions. The significant decrease in SO_2 concentrations in winter is beneficial to health given that the concentration of SO_2 usually exceeds the health-based critical value in winter. On average, the concentration of SO_2 in summer is reduced by 45%, which might help reduce the formation of secondary aerosols under the active photochemical reaction.

Besides the change in source emissions, the variation of SO_2 concentration also depends on weather conditions, atmospheric diffusion, transmission, and photochemical reactions. These factors can be different year by year, and thus affect the comparability of SO_2 concentrations in the different periods. In Beijing urban area, surface SO_2 concentration is mainly determined by local SO_2 emissions, but it also can be affected by the transport of external SO_2. The variation of wind speed and direction is usually associated with atmospheric dispersion and transport. Temperature is one of the most important factors which could affect the chemical reactions in the atmosphere. Relative humidity (RH) indicates the relative water content in the atmosphere, and it's closely associated with the weather pattern. For example, the humidity in rainy or cloudy days is normally higher than that in sunny days. Therefore, the meteorological conditions influence the lifetime and transport of SO_2. To minimize the meteorological effects, the data before, during, and after the Olympics are reclassified according to temperature, RH wind speed and wind direction. The average mixing ratios of SO_2 for different intervals are calculated. In this way, the mean reduction of SO_2 for different meteorology classes in the pre-Olympics and post-Olympics periods can be determined.

Figure 10 shows the mixing ratios of SO_2 during the pre-Olympic and the post-Olympic period as a function of RH, wind speed, wind direction and temperature at CMA. It can be seen in Fig. 10 that SO_2 concentrations during the pre-Olympic period are higher than those during the post-Olympic period at RH of greater than 30%, at a wind speed of less than 5 m/sec, and within most of the temperature range. At NNW-N-NE sector and W-SW-S sector, SO_2 concentrations during the pre-Olympics are significantly higher than those during the post-Olympics.

At CMA, the concentration of SO_2 increases with the increasing RH when RH is less than 40%, and decrease with the increasing RH when RH is greater than 40%. The mean RH (<40%) is 25.6% and 24.8% during the pre-Olympics and the post-Olympics, respectively. Under the condition of RH > 40%, the difference between the concentrations of SO_2 in the pre-Olympics and post-Olympics is remarkable. More than 82% of RH data from CMA lie within 20%–90%, In this RH range, the average RH values in the pre-Olympics and post-Olympics are 50.3% and 49.1%, respectively, and the average concentrations of SO_2 in the pre-Olympics and post-Olympics are 21.6 and 14.4 ppb, respectively, with a decrease of 33%. The 59% of RH data lie within 40%–90%. In this RH range, the average RH values in the pre-Olympics and post-Olympics are 64.3% and 62.4%, respectively, and the average concentrations of SO_2 in the pre-Olympics and post-Olympics are 22.7 and 13.7 ppb, respectively, with a decrease of 42%. Clearly, the change in RH is not the major factor causing the significant difference of SO_2 during the pre-Olympics and the post-Olympics.

The concentration of SO_2 at CMA decreases with increasing wind speed (WS). The average WS are 2.1 and 2.3 m/sec during the pre-Olympics and the post-Olympics, respectively. More than 87% of observed WS at CMA are less than 4 m/sec. In this WS range, the WS averages 1.74 m/sec both in the pre-Olympics and in post-Olympics, and the mean levels of SO_2 in the pre-Olympics and post-Olympics are 19.1 and 14.5 ppb, respectively, with a decrease of 24%. The 78% of observed WS at CMA are less than 3 m/sec. In this WS range, the average WS values in the pre-Olympics and post-Olympics are 1.5 and 1.53 m/sec, respectively, and the mean levels of SO_2 in the pre-Olympics and post-Olympics are 21.6 and 15.3 ppb, respectively, with a decrease of 29%. Therefore, the change of WS is also not the major factor causing the significant difference of SO_2 during the pre-Olympics and the post-Olympics.

High RH often corresponds to low WS. Under the condition of high RH and low WS, which show more features of local air condition, the reduction of SO_2 is

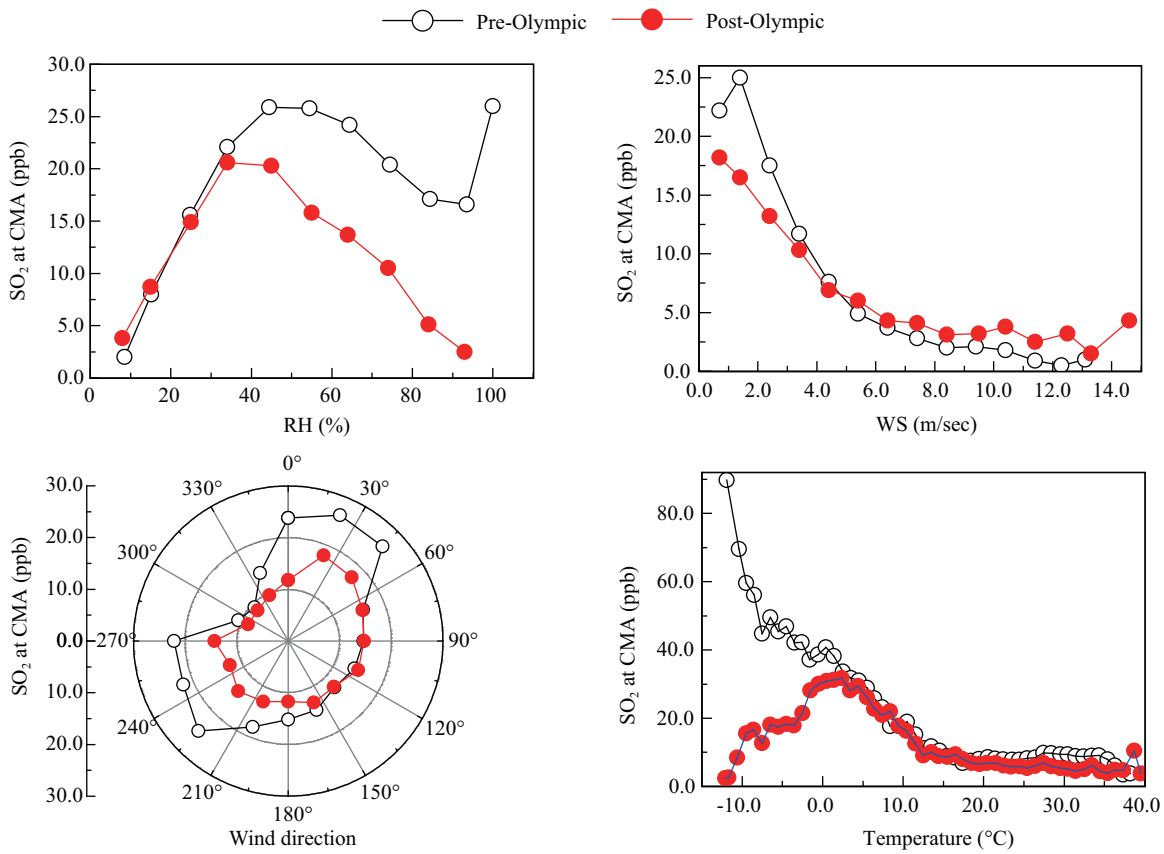

Fig. 10 Mixing ratios of SO_2 in the pre-Olympics and post-Olympics as a function of relative humidity (RH), wind speed (ws), wind direction and temperature at CMA.

more significant. The 59% and 50% of SO_2 data are collected under RH ≥ 40% and WS ≤ 3 m/sec in the pre-Olympics and post-Olympics periods, respectively. The average concentrations of SO_2 in the pre-Olympics and post-Olympics under such conditions are 22.5 and 13.6 ppb, respectively.

The difference between the SO_2 concentrations during the pre-Olympics (21.3 ppb) and the post-Olympics (13.5 ppb) is significant when the wind comes from the northeast and southwest sectors. The number of data obtained under this wind condition accounts for 69% of the total number of data. In other wind sectors, the concentrations of SO_2 in the post-Olympics are not much lower than those in the pre-Olympics, probably reflecting the sector differences in the distribution of major SO_2 sources and the effectiveness of SO_2 emission reduction.

The overall average ambient temperatures are 13.7 and 14.6°C during the pre-Olympics and the post-Olympics, respectively. When the ambient temperature is less than 3°C (mainly in winter), the average temperatures in the pre-Olympics and post-Olympics are –1.7 and –1.2°C, respectively, and the mean SO_2 concentrations during the pre-Olympics and the post-Olympics are 43.0 and 21.5 ppb, respectively. When the ambient temperature is within 20–34°C (mainly in summer), the average temperatures in the pre-Olympics and post-Olympics are 25.8 and 25.6°C, respectively, and the mean SO_2 concentrations during the pre-Olympics and the post-Olympics are 8.7 and 6.0 ppb, respectively. The average decrease of SO_2 in winter and summer is 35%. But, there is no significant difference in SO_2 when the temperature is within 3–19°C. The different reductions of SO_2 in different temperature ranges may reflect the different variations of SO_2 in different seasons, as shown in Fig. 9a. The SO_2 concentrations are normally high in winter and low in summer, and there are significant changes of SO_2 in summer and winter, but not in spring and fall. In the pre-Olympics, the concentrations of SO_2 decreased with increasing temperature, but in post-Olympics, the concentrations of SO_2 increased first and then decreased with increasing temperature, which may reflect the significant change of high value of SO_2 in winter. Therefore, the change of temperature is also not the major factor causing the significant difference in SO_2 during the pre-Olympics and the post-Olympics.

Based on the above discussion, the 35% difference between the SO_2 concentrations at CMA in the pre-Olympics and the post-Olympics periods are caused by significant decrease in the occurrence of high SO_2 concentration, which is likely to be related with reduction measures of SO_2 emission and has little to do with year-to-year changes in meteorological conditions.

3.2.3 Changes of SO_2 at GCH

Figure 11 shows the monthly mean and the frequency distribution of hourly mean of SO_2 before, during and after the Olympics at GCH. The annual average concentrations of SO_2 are (18.9 ± 12.9) ppb during the pre-Olympics and (12.1 ± 7.7) ppb during the post-Olympics. The greatest decrease in the absolute SO_2 concentrations appeared in winter (DJF) with a reduction of 16.2 ppb (42%), and then

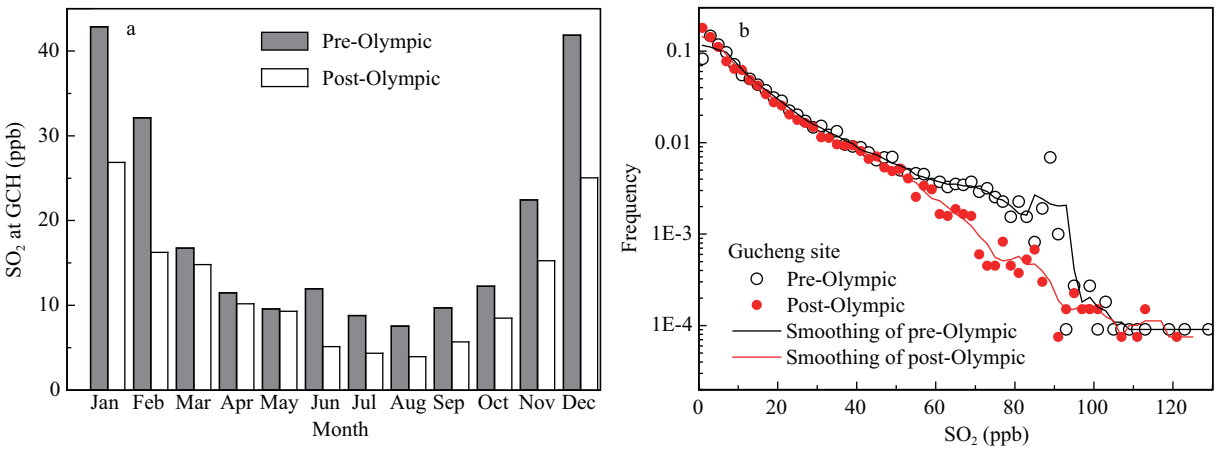

Fig. 11 The monthly mean (a) and the frequency distribution of hourly mean (b) of SO_2 before and during/after the Olympics at GCH.

in summer (JJA) and autumn (SON), together with a reduction of 5.0 ppb (43%; and 48% in August). The smallest decrease in the absolute SO_2 concentrations appeared in spring (MAM) with a reduction of 1.2 ppb (8.5%) and no obvious change appeared in May. The frequency of high SO_2 concentrations (>50 ppb) was also significantly reduced (Fig. 11b).

Figure 12 shows the mixing ratios of SO_2 during the pre-Olympics and post-Olympics as a function of RH, wind speed, wind direction and temperature at GCH. As can be seen in Fig. 12, the difference between the concentrations of SO_2 during the pre-Olympics and post-Olympics is remarkable when RH > 40%. The 89% of RH values at GCH lie within 30%–99%. In this RH range, the average RH values in the pre-Olympics and post-Olympics are 71% and 68%, respectively, and the mean SO_2 concentrations during the pre-Olympics and the post-Olympics are 18.0 and 13.9 ppb, respectively. The 81% of RH values lie within 40%–99%. In this RH range, the average RH values in the pre-Olympics and post-Olympics are 74% and 72%, respectively, and the mean SO_2 concentrations during the pre-Olympics and post-Olympics are 17.8 and 12.9 ppb, respectively. Similar to that at CMA, the SO_2 concentration increases with the increase of RH under RH < 40%, and decreases with the increase of RH under RH > 40%. The average SO_2 concentration under RH > 40% is

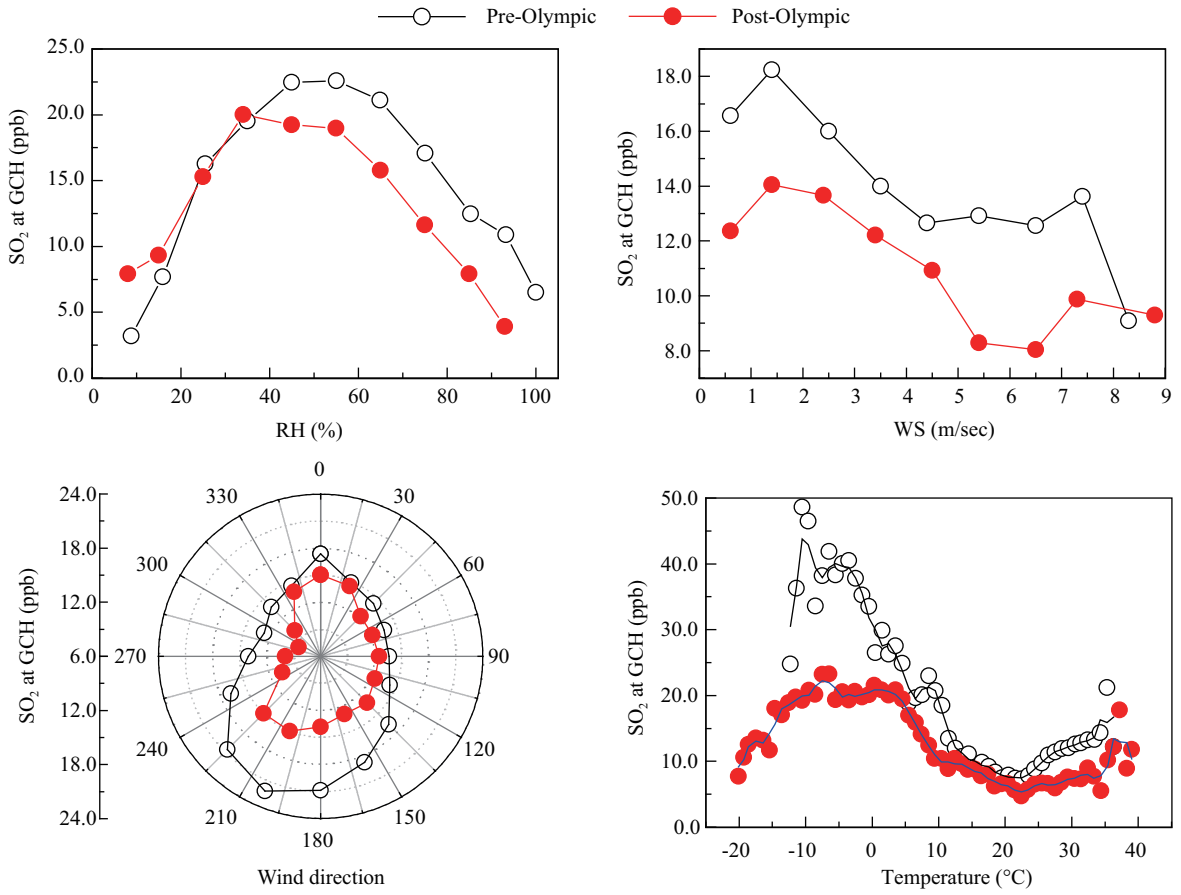

Fig. 12 Mixing ratios of SO_2 during the pre-Olympics and the post-Olympics as a function of RH, WS, wind direction and temperature at GCH.

higher during the pre-Olympics than that during the post-Olympics.

The 86% of measured WS at GCH is less than 3 m/sec. Under this wind condition, the WS averages 1.2 m/sec both in the pre-Olympics and in post-Olympics, and the mean SO_2 concentrations during the pre-Olympics and the post-Olympics are 16.9 and 13.4 ppb, respectively. The 99% of measured WS is less than 6 m/sec. Under this wind condition, the WS averages 1.6 m/sec both in the pre-olympics and in post-Olympics, and the mean SO_2 concentrations during the pre-Olympics and the post-Olympics are 15.1 and 11.9 ppb, respectively. The average WS during the pre-Olympics is the same as that during the post-Olympics.

The difference in SO_2 concentrations during the pre-Olympics (18.5 ppb) and the post-Olympics (12.9 ppb) are significant when the wind comes from the southern sector. The fractions of those data are 41% and 44% of the total data in the pre-Olympics and post-Olympics, respectively. The concentrations of SO_2 from the southern sector at GCH are often higher than those in other sectors, so the significant reduction of SO_2 from south sector coincides with the effective control of SO_2 emission in the major polluted area.

At GCH, the average temperature is 15.3 and 10.7°C during the pre-Olympics and the post-Olympics, respectively. In the temperature range from –13 to 5°C, the average temperatures in the pre-Olympics and post-Olympics are –1.4 and –2.0°C, respectively, and the mean SO_2 concentrations are 35.0 and 20.4 ppb during the pre-Olympics and the post-Olympics, respectively. In the temperature range of 11–27°C, the average temperatures in the pre-Olympics and post-Olympics are 20.5 and 19.5°C, respectively, and the mean SO_2 concentrations are 9.5 and 7.3 ppb during the pre-Olympics and the post-Olympics, respectively. In the other temperature range, the mean SO_2 concentrations are 15.9 and 9.8 ppb in the pre-Olympics and post-Olympics, respectively. Overall, the average decrease is 32%. Similar to that at CMA, the concentrations of SO_2 decrease with the increase of temperature during the post-Olympics, but the concentrations of SO_2 increase first and then decrease with the increase of temperature during the post-Olympics, reflecting a significant change in the occurrence of high value of SO_2 in winter.

3.2.4 Changes of SO_2 at SDZ

Figure 13 shows the monthly average and the frequency distribution of hourly mean of SO_2 concentrations before, during and after the Olympics at SDZ. The maximum relative deviation of SO_2 is found in June (42%), followed by that in April (38%). The annual average concentrations of SO_2 are (7.7 ± 4.1) ppb during the pre-Olympics and (6.7 ± 4.0) ppb during the post-Olympics. The difference between SO_2 concentrations at SDZ in the pre-Olympics and post-Olympics periods is obvious only in some months, e.g., March–June. SDZ locates at the north edge of the North China Plain, to the south of which is the relatively polluted region and to the north of which are very clean mountainous and hilly areas (Lin et al., 2008). Air transport from different regions can bring different levels of pollutants to SDZ (Lin et al., 2008; Xu et al., 2009b). SDZ is more influenced by polluted air from the south in warmer months and by clean air from the north in colder months. Because the control measures aim mainly at the major emission source in polluted areas, the effect is not readily seen at SDZ.

Figure 14 shows the mixing ratios of SO_2 in the pre-Olympics and post-Olympics as a function of RH, wind speed, wind direction and temperature at SDZ. As shown in Fig. 14, the greatest difference between SO_2 concentrations at SDZ in the pre-Olympics and post-Olympics periods is observed under the conditions of relatively low humidity and high wind speed, which is different from those at GCH and CMA. At SDZ, the surface SO_2 concentration usually increases with the increase of WS (2–8 m/sec), which is also different from those at CMA and GCH. The 69% of measured RH at SDZ is less than 70%. Under this humidity condition, the RH averages 39% both in the pre-Olympics and in post-Olympics, and the mean SO_2 concentrations in the pre-Olympics and post-Olympics are 8.1 and 6.1 ppb, respectively. The 61% of WS values at SDZ lie in the range of 2–8 m/sec. In this WS range, the average WS values in the pre-Olympics and post-Olympics are 2.6 and 3.5 m/sec, respectively, and the average concentrations of SO_2 in the pre-Olympics and post-Olympics are 10.0 and 7.8 ppb, respectively. The

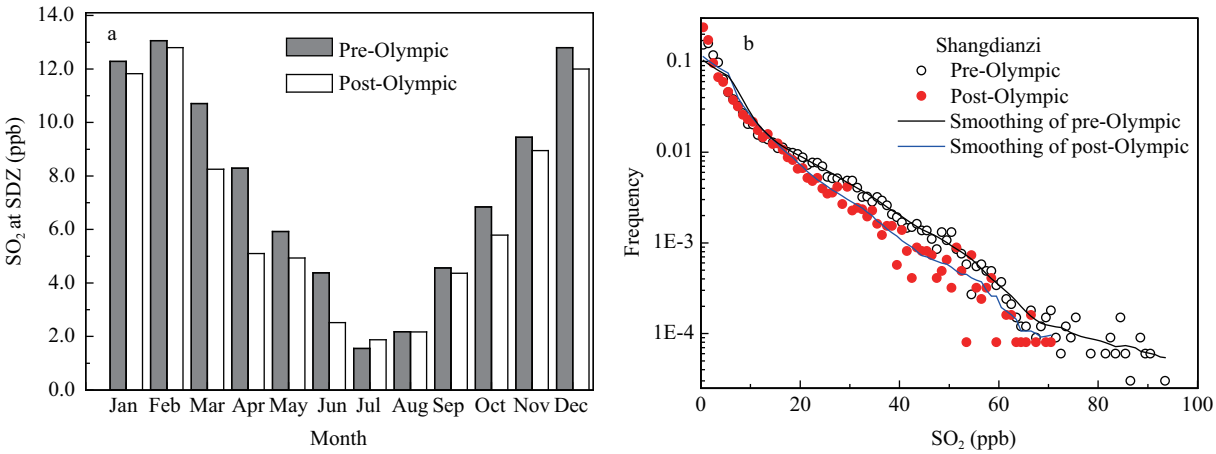

Fig. 13 Monthly mean (a) and the frequency distribution of hourly mean (b) of SO_2 before and during/after the Olympics at SDZ.

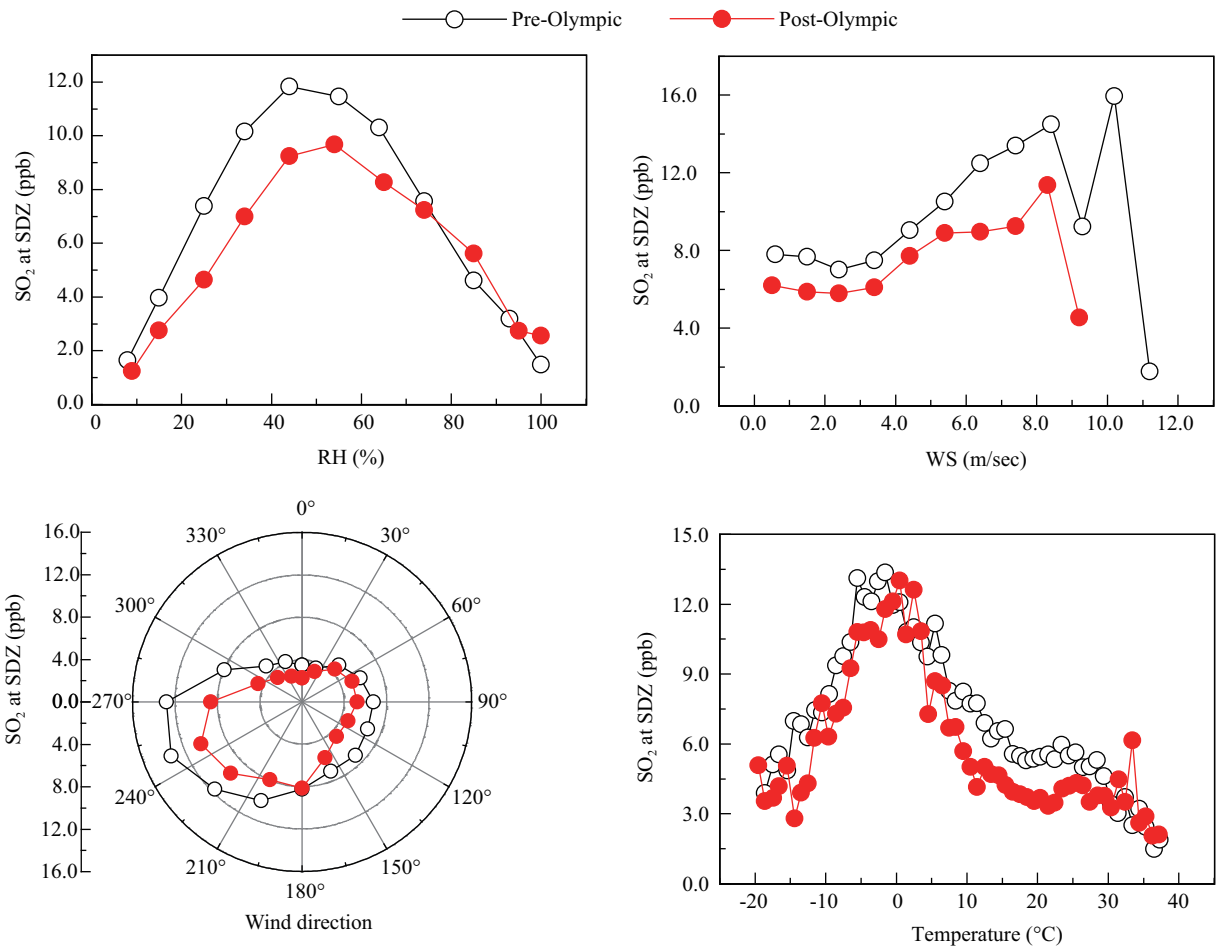

Fig. 14 Mixing ratios of SO_2 during pre-Olympics and post-Olympics as a function of RH, WS, wind direction and temperature at SDZ site.

38% of WS values at SDZ is less than 2 m/sec. In this WS range, the average WS values in the pre-Olympics and post-Olympics are 1.2 and 1.1 m/s, respectively, and the mean values of SO_2 in the pre-Olympics and post-Olympics are 7.7 and 6.0 ppb, respectively. The low RH and high WS conditions favor atmospheric mixing and transport, leading to more regional pollution. Under the condition of RH ≤ 70% and WS ≥ 2 m/sec, the mean values of SO_2 in the pre-Olympics and post-Olympics are 8.6 and 6.9 ppb, respectively.

The difference between SO_2 concentrations in the pre-Olympics (11.2 ppb) and post-Olympics (8.2 ppb) are significant when the wind comes from the W-WSW-SW sector. The fractions of those data are 36.1% and 36.7% of the total data in the pre-Olympics and post-Olympics, respectively. The W-WSW-SW sector of SDZ corresponds to the southwest mouth of the canyon towards to Beijing (Lin et al., 2008), thus the concentrations of SO_2 in this sector are much higher than those in other sectors as discussed in Lin et al. (2008) and Meng et al. (2009). When wind comes from the southeast sector, the mean values of SO_2 are 6.9 and 5.1 ppb in the pre-Olympics and post-Olympics, respectively. The difference in SO_2 concentrations is very small when wind comes from the clean northern sector (especially from the northeast). The change of the SO_2 level (27%) under southwest winds is mainly due to the reduction of the SO_2 emission in Beijing and its surrounding areas.

In the temperature range of 4–30°C, the average temperatures in the pre-Olympics and post-Olympics are 17.1 and 17.5°C, respectively, and the mean values of SO_2 in the pre-Olympics and post-Olympics are 6.6 and 4.8 ppb, respectively, with a decrease of 27%. In other temperature ranges, the difference is small, with the mean temperatures being 10.5 and 10.8°C in the pre-Olympics and post-Olympics, respectively.

4 Discussion and conclusions

The observations of SO_2 in recent years in North China region show that the average concentrations of SO_2 at CMA (Beijing urban area), GCH (relatively polluted rural area), and SDZ (regional background area) are (16.8 ± 13.1) ppb, (14.8 ± 9.4) ppb, and (7.5 ± 4.0) ppb, respectively. The SO_2 levels in winter (heating season) are 4–6 folds higher than those in summer. There are significant correlations among daily mean concentrations of SO_2 at different sites, reflecting the regional characteristics of SO_2 over North China. The average diurnal variations of SO_2 at the above sites show a common feature of daytime peak, which is either higher or equal to nocturnal SO_2 peak. Such daytime peak is not intuitively understandable, given the short lifetime of SO_2. In view of the topography-related prevailing winds in the North China Plain region and

existence of elevated layer of high SO_2 over the region, we believe that the daytime SO_2 peak is caused by advection transport and/or downward mixing of SO_2-richer air.

Our data from recent years show highly significant (P <0.0001) decrease trends of surface SO_2 at CMA (–4.4 ppb/yr) and GCH (–2.4 ppb/yr), reflecting the effectiveness of SO_2 emission control in Beijing and its surrounding areas. However, at SDZ, a regional atmospheric background site in the North China region, only a minor downward trend (–0.3 ppb/yr) of surface SO_2 is found. This suggests that the small SO_2 decrease (1–2 ppb/yr) before 2008 Beijing Olympic Games in the major source area (Beijing urban area) has only a limited impact on the regional background concentration of SO_2. In addition, a slight trend of SO_2 at SDZ may be masked by varying weather and atmospheric transport conditions and by the urbanization expanding towards the rural areas, which can change the distribution of SO_2 sources.

Because of Beijing 2008 Olympic Games, strict emission control measures were carried out in Beijing and its surrounding areas. The SO_2 concentrations of different sites have largely reduced after all the measures, suggesting that the SO_2 pollution control for the Olympics has a long-lasting effect. In the post-Olympics period, the mean concentrations of SO_2 at CMA, GCH, and SDZ are (14.3 ± 11.0) ppb, (12.1 ± 7.7) ppb, and (7.5 ± 4.0) ppb, respectively, corresponding to the reductions of 26%, 36%, and 13% from the pre-Olympics period, respectively. Statistical analysis on the mixing ratio of SO_2 with meteorological parameters shows that the differences of temperature, relative humidity, wind speed, and wind direction before and after the Olympic Games were not the dominant factors leading to significant difference of SO_2 in the pre-Olympics and post-Olympics.

If only considering the data with more representativeness of the local characteristic in Beijing urban area, such as the observational data under the conditions of RH≥40% and WS≤3 m/sec, we obtain a 40% reduction of the SO_2 concentration at CMA after the control measures for the Olympic Games, which is higher than the overall decrease of 26%. This fact suggests that the impact of SO_2 transport from surrounding areas of Beijing cannot be ignored. The change of SO_2 at CMA from the pre-Olympics to post-Olympics is mainly caused by the significant decrease of the occurrence of high SO_2 events and the significant reduction (37%) of SO_2 in winter and in the wind directions of high SO_2, indicating the effective control of major SO_2 pollution sources or regions. Similar results are obtained for GCH. Obviously, the reduction of extreme pollution events will benefit health of residents in the region.

Unlike the decreases of SO_2 at GCH and CMA, larger decreases of SO_2 at SDZ from the pre-Olympics to post-Olympics period occur under the conditions of relatively low humidity and high wind speed, under which atmospheric mixing and transport are better and hence SO_2 is more regionally distributed. Using the data under RH≤70% and WS≥2 m/sec, which reflect better the regional situation, a SO_2 reduction of 20% from the pre-Olympics to post-Olympics period is calculated, which is higher than the overall decrease of 13%. The SO_2 levels associated with winds from the clean northern sector (especially from northeast) show very small decreases, while those associated with winds the southwest sector show an average SO_2 decrease of 27%, presumably due to the large reduction of SO_2 emission in Beijing and its surrounding areas.

In summary, the emission control measures implemented for Beijing 2008 Olympic Games are very effective and have caused 20%–40% reductions of ambient SO_2 at different sites in Beijing and its surrounding areas. The effect of SO_2 pollution control is not limited to the Olympic Games period, but measurable also after that. To maintain long-lasting benefits, it is crucial to further strictly control the SO_2 emissions.

Acknowledgments

We thank the operators of the Shangdianzi, Gucheng and China Meteorological Administration stations for carrying out the measurements. This work is supported by the National Basic Research Program of China (No. 2005CB4222002), the National Natural Science Foundation of China (No. 20407001, 40775074), the Basic Research Fund of CAMS (No. 2008Z011, 2011CX001, 2011Z003) and the China Meteorological Administration (No. GYHY200706036, GYHY201106050).

References

Alexander B, Park R J, Jacob D J, Li Q B, Yantosca R M, Savarino J et al., 2005. Sulfate formation in sea-salt aerosols: Constraints from oxygen isotopes. *Journal of Geophysical Research*, 110: D10307. DOI: 10.1029/2004JD005659.

Carmichael G R, Streets D G, Calori G, Amann M, Jacobson M Z, Hansen J et al., 2002. Changing trends in sulfur emissions in Asia: Implications for acid deposition, air pollution, and climate. *Environmental Science & Technology*, 36(22): 4707–4713.

Chen Y, Zhao C S, Zhang Q, Deng Z Z, Huang M Y, Ma X C, 2009. Aircraft study of mountain chimney effect of Beijing, China. *Journal of Geophysical Research*, 114: D08306. DOI: 10.1029/2008JD010610.

Ding A, Wang T, Xue L, Gao J, Stohl A, Lei H et al., 2009. Transport of north China air pollution by midlatitude cyclones: Case study of aircraft measurements in summer 2007. *Journal of Geophysical Research*, 114: D08304. DOI: 10.1029/2008JD011023.

Fiedler V, Arnold F, Schlager H, Dörnbrack A, Pirjola L, Stohl A, 2009. East Asian SO_2 pollution plume over Europe – Part 2: Evolution and potential impact. *Atmospheric Chemistry and Physics*, 9: 4729–4745.

Hao J M, Wang L T, 2005. Improving urban air quality in China: Beijing case study. *Journal of the Air and Waste Management Association*, 55(9): 1298–1305.

Ji D S, Wang Y S, Sun Y, Ma Z Q, 2009. Characteristics of atmospheric SO_2 in Beijing. *Climatic and Environmental Research*, 14(1): 69–76.

Kaufman Y J, Tanré D, Boucher O, 2002. A satellite view of aerosols in the climate system. *Nature*, 419(6903): 215–223.

Kiehl J T, Briegleb B P, 1993. The relative roles of sulfate aerosols and greenhouse gases in climate forcing. *Science*,

260(5106): 311–314.

Krotkov N A, Carn S A, Krueger A J, Bhartia P K, Yang K, 2006. Band residual difference algorithm for retrieval of SO_2 from the aura ozone monitoring instrument (OMI). *IEEE Transactions on Geoscience and Remote Sensing*, 44(5): 1259–1266.

Larssen T, Lydersen E, Tang D G, He Y, Gao J X, Liu H Y et al., 2006. Acid rain in China, rapid industrialization has put citizens and ecosystems at risk. *Environmental Science & Technology*, 40(2): 418–425.

Lee C, Richter A, Lee H, Kim Y J, Burrows J P, Lee Y G et al., 2008. Impact of transport of sulfur dioxide from the Asian continent on the air quality over Korea during May 2005. *Atmospheric Environment*, 42(7): 1461–1475.

Lin W L, Xu X B, Ge B Z, Zhang X C, 2009. Characteristics of gaseous pollutants at Gucheng, a rural site southwest of Beijing. *Journal of Geophysical Research*, 114: D00G14. DOI: 10.1029/2008JD010339.

Lin W, Xu X, Zhang X, Tang J, 2008. Contributions of pollutants from North China Plain to surface ozone at the Shangdianzi GAW Station. *Atmospheric Chemistry and Physics*, 8(19): 5889–5898.

Lin W L, Xu X B, Zhang X C, 2011a. The errors in the claimed concentrations of standard gases used in the observation of reactive gases and recommended solutions. *Environmental Chemistry*, 30(6): 1–4.

Lin W, Xu X, Ge B, Liu X, 2011b. Gaseous pollutants in Beijing urban area during the heating period 2007–2008: variability, sources, meteorological, and chemical impacts. *Atmospheric Chemistry and Physics*, 11: 8157–8170.

Liu J, Zhang X L, Xu X F, Xu H H, 2008. Comparison analysis of variation characteristics of SO_2, NOx, O_3 and $PM_{2.5}$ between rural and urban areas, Beijing. *Environmental Science*, 29(4): 1059–1065.

Lu Z, Streets D G, Zhang Q, Wang S, Carmichael G R, Cheng Y F et al., 2010. Sulfur dioxide emissions in China and sulfur trends in East Asia since 2000. *Atmospheric Chemistry and Physics*, 10(13): 6311–6331.

Manktelow P T, Carslaw K S, Mann G W, Spracklen D V, 2009. Variable CCN formation potential of regional sulfur emissions. *Atmospheric Chemistry and Physics*, 9(10): 3253–3259.

Meng X Y, Wang P C, Wang G C, Yu H, Zong X M, 2009. Variation and transportation characteristics of SO_2 in winter over Beijing and its surrounding areas. *Climatic and Environmental Research*, 14(3): 309–317.

Meng Z Y, Ding G A, Xu X B, Xu X D, Yu H Q, Wang S F, 2008. Vertical distributions of SO_2 and NO_2 in the lower atmosphere in Beijing urban areas, China. *Science of the Total Environment*, 390(2-3): 456–465.

Meng Z Y, Xu X B, Yan P, Ding G A, Tang J, Lin W L et al., 2009. Characteristics of trace gaseous pollutants at a regional background station in Northern China. *Atmospheric Chemistry and Physics*, 9(3): 927–936.

Mitchell J F B, Johns T C, Gregory J M, Tett S F B, 1995. Climate response to increasing levels of greenhouse gases and sulphate aerosols. *Nature*, 376(6540): 501–504.

Ravishankara A R, 1997. Heterogeneous and multiphase chemistry in the troposphere. *Science*, 276(5315): 1058–1065.

Seinfeld J H, Pandis S N, 2006. Atmospheric Chemistry and Physics – From Air Pollution to Climate Change (2nd ed.). John Wiley and Sons.

Shao M, Tang X Y, Zhang Y H, Li W J, 2006. City clusters in China: air and surface water pollution. *Frontiers in Ecology and the Environment*, 4(7): 353–361.

Slanina S (Lead Author); Davis W (Topic Editor), 2008. "Air pollution emissions." In: Encyclopedia of Earth (Cleveland C J, ed.). Environmental Information Coalition, National Council for Science and the Environment. http://www.eoearth.org/article/Air_pollution_emissions, Washington DC.

Stern D I, 2005: Global sulfur emissions from 1850 to 2000. *Chemosphere*, 58(2): 163–175.

Streets D G, Waldhoff S T, 2000. Present and future emissions of air pollutants in China: SO_2, NOx, and CO. *Atmospheric Environment*, 34(3): 363–374.

Sun Y, Wang Y S, Liu G R, An J L, Ma Z Q, Shi L Q et al., 2006. Analysis for vertical profile of atmospheric SO_2 during air seriously polluted days in Beijing. *Environmental Sciences*, 27(3): 407–414.

Sun Y, Wang Y S, Zhang C C, 2009. Measurement of the vertical profile of atmospheric SO_2 during the heating period in Beijing on days of high air pollution. *Atmospheric Environment*, 43(2): 468–472.

Tang D G, Liu H J, Wang W, Wang M Y, Cui P, Du J, 2000. Aircraft measurement of atmospheric pollutants in winter in North China I: research on pollution properties of gaseous pollutants. *Research of Environmental Sciences*, 13(1): 6–9.

Tang J, Xu X B, Ba J, Wang S F, 2007. Trend of precipitation acidity in Beijing–Tianjin region: the implication of particle abatement effort rends of the precipitation acidity over China during 1992–2006. *Journal of the Graduate School of the Chinese Academy of Sciences*, 24(5): 667–673.

Tang J, Xu X B, Ba J, Wang S F, 2010. Trends of the precipitation acidity over China during 1992–2006. *Chinese Science Bulletin*, 55(17): 1800–1807.

Thornton D C, Bandy A R, Blomquist B W, Talbot R W, Dibb J E, 1997. Transport of sulfur dioxide from the Asian Pacific Rim to the North Pacific troposphere. *Journal of Geophysical Research*, 102(D23): 28489–28499.

Wang W X, Ding G A, 1997. The geographical distribution of ion concentration in precipitation over China. *Research of Environmental Sciences*, 10(2): 1–6.

Wang W X, Wang T, 1995. On the origin and the trend of acid precipitation in China. *Water, Air and Soil Pollution*, 85(4): 2295–2300.

Wang Y, Hao J, McElroy M B, Munger J W, Ma H, Chen D et al., 2009. Ozone air quality during the 2008 Beijing Olympics: effectiveness of emission restrictions. *Atmospheric Chemistry and Physics*, 9(14): 5237–5251.

Wang S, Zhao M, Xing J, Wu Y, Zhou Y, Lei Y et al., 2010. Quantifying the air pollutants emission reduction during the 2008 Olympic Games in Beijing. *Environmental Science & Technology*, 44(7): 2490–2496.

Ward P L, 2009. Sulfur dioxide initiates global climate change in four ways. *Thin Solid Films*, 517(11): 3188–3203.

WHO, 2000. Air Quality Guidelines for Europe (2nd ed.). WHO Regional Publications, European Series, No. 91.

Xu W Y, Zhao C S, Ran L, Deng Z Z, Liu P F, Ma N et al., 2011. Characteristics of pollutants and their correlation to meteorological conditions at a suburban site in the North China Plain. *Atmospheric Chemistry and Physics*, 11(9): 4353–4369.

Xu X B, Lin W L, Yan P, Zhang Z, Yu X M, 2009a. Long-term changes of acidic gases in China's Yangtze Delta and Northeast Plain Regions during 1994–2006. *Advance in Climate Change Research*, 5(Suppl.): 5–10.

Xu X B, Liu X W, Lin W L, 2009b. Impacts of air parcel transport

on the concentrations of trace gases at regional background stations. *Journal of Applied Meteorological Science*, 20(6): 656–664.

Xu X D, Shi X H, Xie L, Ding G A, Miao Q J, Ma J Z et al., 2005. Spatial character of the gaseous and particulate state compound correlation of urban atmospheric pollution in winter and summer. *Science in China Earth Science*, 48(Supp. II): 64–79.

Xue L, Ding A, Gao J, Wang T, Wang W, Wang X et al., 2010. Aircraft measurements of the vertical distribution of sulfur dioxide and aerosol scattering coefficient in China. *Atmospheric Environment*, 44(2): 278–282.

Zhang J, Miao H, Ouyang Z Y, Wang X K, 2006. Ambient air quality trends and driving factor analysis since 1980's in Beijing. *Acta Scientiae Circumstantiae*, 26(11): 1886–1892.

Zhang Q, Streets D G, Carmichael G R, He K B, Huo H, Kannari A et al., 2009. Asian emissions in 2006 for the NASA INTEX-B mission. *Atmospheric Chemistry and Physics*, 9(14): 5131–5153.

Zhang X Y, Wang Y Q, Lin W L, Zhang Y M, Zhang X C, Gong S et al., 2009. Changes of Atmospheric compositions and optical property over Beijing: 2008 Olympic monitoring campaign. *Bulletin of the American Meteorological Society*, 90(11): 1633–1651.

Zhao Y X, Hou Q, 2010. Characteristics of the acid rain variation in China during 1993–2006 and associated causes. *Acta Meteorologica Sinica*, 24(2): 239–250.